

Reduced Biosynthesis of Digalactosyldiacylglycerol, a Major Chloroplast Membrane Lipid, Leads to Oxylipin Overproduction and Phloem Cap Lignification in *Arabidopsis*^{OPEN}

Yang-Tsung Lin,^a Lih-Jen Chen,^a Cornelia Herrfurth,^b Ivo Feussner,^{b,c} and Hsou-min Li^{a,1}

^a Institute of Molecular Biology, Academia Sinica, Taipei 11529, Taiwan

^b Georg-August-University Goettingen, Albrecht-von-Haller-Institute for Plant Sciences, Department of Plant Biochemistry, D-37077 Goettingen, Germany

^c Georg-August-University Goettingen, Goettingen Center for Molecular Biosciences, Department of Plant Biochemistry, D-37077 Goettingen, Germany

ORCID IDs: 0000-0001-8826-4251 (Y.-T.L.); 0000-0002-9888-7003 (I.F.); 0000-0002-0211-7339 (H.-m.L.)

DIGALACTOSYLDIACYLGLYCEROL SYNTHASE1 (DGD1) is a chloroplast outer membrane protein responsible for the biosynthesis of the lipid digalactosyldiacylglycerol (DGDG) from monogalactosyldiacylglycerol (MGDG). The *Arabidopsis thaliana* *dgd1* mutants have a greater than 90% reduction in DGDG content, reduced photosynthesis, and altered chloroplast morphology. However, the most pronounced visible phenotype is the extremely short inflorescence stem, but how deficient DGDG biosynthesis causes this phenotype is unclear. We found that, in *dgd1* mutants, phloem cap cells were lignified and jasmonic acid (JA)-responsive genes were highly upregulated under normal growth conditions. The *coronative insensitive1 dgd1* and *allene oxide synthase dgd1* double mutants no longer exhibited the short inflorescence stem and lignification phenotypes but still had the same lipid profile and reduced photosynthesis as *dgd1* single mutants. Hormone and lipidomics analyses showed higher levels of JA, JA-isoleucine, 12-oxo-phytodienoic acid, and arabidopsides in *dgd1* mutants. Transcript and protein level analyses further suggest that JA biosynthesis in *dgd1* is initially activated through the increased expression of genes encoding 13-lipoxygenases (LOXs) and phospholipase A-1γ3 (At1g51440), a plastid lipase with a high substrate preference for MGDG, and is sustained by further increases in LOX and allene oxide cyclase mRNA and protein levels. Our results demonstrate a link between the biosynthesis of DGDG and JA.

INTRODUCTION

The galactolipids monogalactosyldiacylglycerol (MGDG) and digalactosyldiacylglycerol (DGDG), the major lipids of chloroplast membranes, are important for photosynthesis and are completely absent in most nonphotosynthetic organisms (Härtel et al., 1997; Dörmann and Benning, 2002; Steffen et al., 2005; Joyard et al., 2010; Boudière et al., 2014; Fujii et al., 2014). MGDG is synthesized by the enzyme MGD synthase, which catalyzes the transfer of a galactose from UDP-galactose onto the diacylglycerol (DAG) backbone. The enzyme DGD synthase then transfers a second galactose from UDP-galactose onto MGDG to form DGDG. Although *Arabidopsis thaliana* is a 16:3 plant and about half of its MGDG molecules have C16 fatty acids at the *sn*-2 position, the predominant fraction of DGDG is derived from the eukaryotic pathway and has C18:3 fatty acids at both the *sn*-1 and *sn*-2 positions (Joyard et al., 2010). In *Arabidopsis*, DGD synthase is encoded by two genes, *DGD1* and *DGD2*. A mutant with a null mutation in the *DGD1* gene, *dgd1*, has been isolated, and its DGDG content was found to be more than 90% lower than in the

wild type (Dörmann et al., 1995), indicating that *DGD1* is the major functional isoform. Studies on *DGD2* have shown that it is mainly involved in DGDG biosynthesis under phosphate-limiting conditions and is also responsible for synthesizing the residual DGDG in the *dgd1* mutant (Kelly and Dörmann, 2002; Kelly et al., 2003).

The *dgd1* mutant has several additional phenotypes. It shows a small reduction in total chlorophyll content and a corresponding reduction in photosynthetic quantum yield. It also has an altered chloroplast morphology, with a rounded envelope enclosing bent thylakoid membranes and large thylakoid-free stromal areas; interestingly, the most pronounced phenotype is stunted growth, in particular, extremely short inflorescence stems, short petioles, and ruffled leaves (Dörmann et al., 1995). Complementation of the *dgd1* single mutant or the *dgd1 dgd2* double mutant with a bacterial glucosyl transferase, thereby replacing DGDG with glucosyl-galactosyl diacylglycerol (GGDG), does not fully rescue the photosynthesis defect, showing that the galactose moiety in DGDG has specific functions in photosynthesis and cannot be replaced by glucose, but the bacterial glucosyl transferase does restore growth and chloroplast morphology (Hözl et al., 2006, 2009). Therefore, it was suggested that the altered chloroplast morphology is the primary cause of growth retardation. However, how an altered chloroplast morphology could result in short inflorescence stems and ruffled leaves is not clear.

Jasmonic acid (JA) is an important hormone for both regular developmental processes, such as pollen maturation, and wound- and pathogen-induced defense responses (Wasternack and

¹ Address correspondence to mbhmli@gate.sinica.edu.tw.

The author responsible for distribution of materials integral to the findings presented in this article in accordance with the policy described in the Instructions for Authors (www.plantcell.org) is: Hsou-min Li (mbhmli@gate.sinica.edu.tw).

^{OPEN}Articles can be viewed without a subscription.

www.plantcell.org/cgi/doi/10.1105/tpc.15.01002

Hause, 2013). JA and its precursors, 12-oxo-phytodienoic acid (OPDA) and dinor-12-oxo-phytodienoic acid (dn-OPDA), belong to the lipid class of oxylipins. JA is synthesized by the allene oxide synthase (AOS) branch of the oxylipin pathway from 18:3 and 16:3 fatty acids released from plastid lipids by lipases (Feussner and Wasternack, 2002), although the identities of these lipases are still a matter of debate (Ellinger et al., 2010; Wasternack and Hause, 2013). The 18:3 and 16:3 fatty acids are sequentially metabolized by lipoxygenase (LOX), AOS, and allene oxide cyclase (AOC) to OPDA and dn-OPDA, respectively, which are exported from the plastids into the peroxisome for the remaining steps of JA biosynthesis. JA is then transported back into the cytosol and is conjugated to the amino acid isoleucine to form the active hormone JA-Ile. The complex of JA-Ile with its receptor CORONATE INSENSITIVE1 (COI1) targets JAZMONATE ZIM DOMAIN transcription repressors for proteasome degradation and induces the expression of genes required for defense signaling and also for a positive feedback response, leading to more JA production (Acosta and Farmer, 2010). In Arabidopsis, an additional pathway may exist for the biosynthesis of OPDA and dn-OPDA, in which the 18:3 and 16:3 acyl chains on galactolipids are directly converted into OPDA and dn-OPDA, producing arabidopsides (galactolipids containing esterified OPDA and dn-OPDA), which are proposed to be storage compounds that allow the rapid release of OPDA and dn-OPDA upon wounding (Mosblech et al., 2009; Acosta and Farmer, 2010; Wasternack and Hause, 2013).

We set out to identify the cause of the reduced inflorescence stem elongation in the *dgd1* mutant and found that the visible phenotypes of *dgd1* were mostly caused by JA overproduction and could be uncoupled from the altered chloroplast morphology. Elevated levels of JA and JA-Ile accumulated in both the *dgd1* single mutants and the *coi1-30 dgd1-1* double mutant lacking the COI1-dependent positive feedback loop, whereas the accumulation of OPDA and arabidopsides was COI1-dependent. Transcript abundance analyses suggested that the initial JA biosynthesis is activated through increased levels of mRNAs coding for LOX and a specific lipase that prefers MGDG as a substrate. High levels of other oxylipins in the *dgd1* single mutants are maintained by further increases in LOX and AOC mRNA and protein levels.

RESULTS

dgd1 Mutants Have Lignified Phloem Cap Cells

To investigate the cause of the short inflorescence stem phenotype (Supplemental Figure 1), we stained stem cross sections of the *dgd1* mutant for lignin with phloroglucinol to allow easy observation of the positions of the xylem and fibers to check for structural abnormalities. We used the previously described *dgd1* mutant allele (Dörmann et al., 1995). We also obtained a new *dgd1* allele (see below); the original allele and the new allele are hereafter referred to as *dgd1-1* and *dgd1-2*, respectively. As shown in Figure 1A, in the wild-type stem, red lignin staining was only detected in the xylem and interfascicular fibers, whereas in the *dgd1-1* mutant, interestingly, an extra group of cells was also lignified. These cells were located at the outermost region of the phloem, immediately

beneath the cortex, and have been referred to as phloem fibers or phloem cap cells (Zhong et al., 2000; Altamura et al., 2001). We followed the latter nomenclature since, in Arabidopsis, these cells are usually large and thin-walled. Because the *dgd1-1* plants also had extremely short petioles compared with the wild type (Supplemental Figure 1), we also stained *dgd1-1* petiole cross sections for lignin and observed lignified phloem cap cells (Figure 1B). To confirm that the lignification phenotype was not restricted to this particular allele, we examined the *dgd1-2* mutant produced by T-DNA insertion (Figure 1C) and found that it had the same short inflorescence stem, short petiole, and ruffled leaf phenotypes (Supplemental Figure 1) and reduced DGDG content (Table 1) as the original mutant. Stem cross sections showed that its phloem cap cells were also lignified (Figure 1A).

Since ectopic lignification in phloem cap cells has been observed in other mutants, including *deetiolated3* (*det3*, encoding V-ATPase subunit C; Newman et al., 2004), *ectopic lignification1* (*eli1*, encoding cellulose synthase CESA3; Caño-Delgado et al., 2003), *broomhead* (encoding eukaryotic release factor eRF1; Petsch et al., 2005), *cpk28* (encoding a calcium-dependent protein kinase; Matschi et al., 2013), *ectopic deposition of lignin in pith1* (*elp1*, encoding a chitinase; Zhong et al., 2000), and *wrky12* (encoding a WRKY transcription factor; Wang et al., 2010), we analyzed the expression of these genes in the *dgd1-1* mutant and found no reduction in expression of any of these genes compared with the wild type (Supplemental Figure 2).

Auxins and Ethylene Are Not the Cause of the *dgd1* Visible Phenotypes

At least three hormones, auxins, ethylene, and JA, have been shown to stimulate secondary cell wall growth or ectopic lignification. Auxins induce xylem differentiation (Fukuda, 2004; Schuetz et al., 2013), and the amount of indole-3-acetonitrile, the precursor of the auxin indole-3-acetic acid, is highly increased in *dgd1-1* (Fiehn et al., 2000). Therefore, we examined whether auxin levels in the phloem cap cell region were higher than in the wild type by crossing into the *dgd1-1* mutant the *DR5-GUS* construct, a reporter gene encoding GUS driven by the synthetic auxin-responsive promoter *DR5* (Ulmasov et al., 1995). In seedling aerial tissues of both wild-type and *dgd1-1* plants (Supplemental Figure 3A, top panels), GUS staining was mainly detected in the periphery of the leaf blades, and no staining was detected in the petioles. In inflorescence stem cross sections of older plants (Supplemental Figure 3A, bottom panels), GUS staining in wild-type plants was mainly detected in the parenchyma cells adjacent to the xylem, while in *dgd1-1* plants, only very faint GUS staining was detected in the same region, and no staining was detected in the phloem cap cell region. This result suggests that auxin levels are not increased in the phloem cap cell region of *dgd1*.

In the *det3* and *eli1* mutants, which show lignification of the phloem cap cells, the ethylene and JA signaling pathways are activated (Caño-Delgado et al., 2003; Brùx et al., 2008). Therefore, we first blocked the ethylene signaling pathway by crossing the *dgd1* mutant with the *ethylene insensitive2* (*ein2*) mutant and found that the double mutant, *dgd1-1 ein2*, was indistinguishable in visible appearance from the *dgd1-1* mutant (Supplemental Figure 3B). Expression of the ethylene-responsive genes *EBP* and

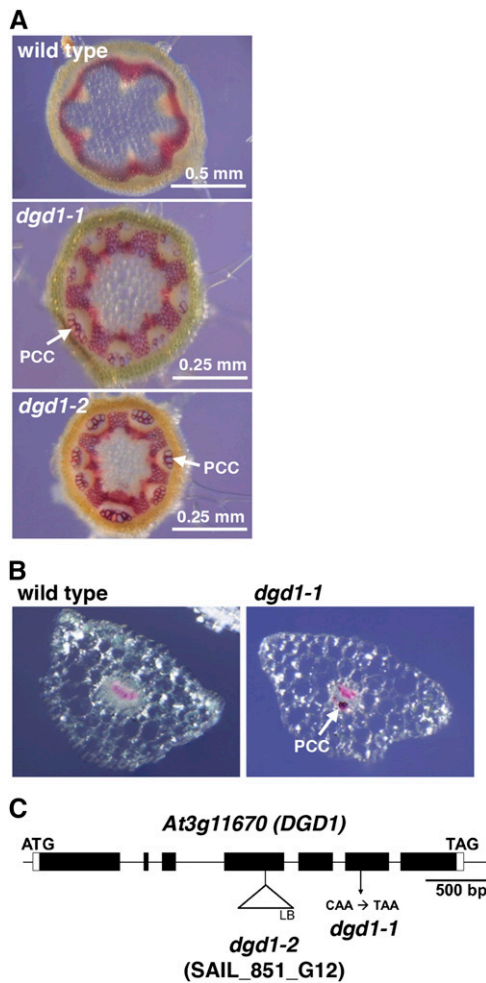


Figure 1. Both of the *dgd1* Mutant Alleles Have Lignified Phloem Cap Cells.

(A) Inflorescence stem cross sections stained with phloroglucinol. Plants were grown for 10 d on MS plates and then transferred to soil for another 25 d. The *dgd1* mutant sections are shown at a 2-fold higher magnification than the wild type. PCC, phloem cap cell.

(B) Petiole cross sections from 40-d-old plants stained with phloroglucinol.

(C) Schematic representation of the mutation positions of the *dgd1-1* and *dgd1-2* alleles. The black boxes, connecting lines between boxes, and white boxes represent, respectively, exons, introns, and the 5' and 3' untranslated regions, respectively.

ETR2 was also not induced in the *dgd1-1* mutant (Supplemental Figure 3C). These results show that activation of the ethylene signaling pathway is not the cause of the *dgd1* phenotypes. We then examined the effect of JA on the mutants.

JA Biosynthesis and JA-Responsive Genes Are Highly Upregulated, and High Levels of Oxylipins Are Seen in *dgd1* under Normal Growth Conditions

JA has been shown to stimulate secondary growth, and exogenous application of JA causes phloem fiber formation (Sehr et al., 2010). Methyl jasmonate treatment of *Arabidopsis* cells results in

the increased expression of genes involved in monolignol biosynthesis and in increased monolignol and oligolignol production (Pauwels et al., 2008). JA biosynthesis has also been shown to be necessary for hypocotyl growth inhibition in the *det3* and *cpk28* mutants (Brüx et al., 2008; Matschi et al., 2015). Furthermore, overexpression of the lipase DONGLE (DGL) results in JA overproduction and generates visible phenotypes of short inflorescence stems and ruffled leaves, very similar to those in *dgd1* (Hyun et al., 2008). Therefore, we examined whether JA signaling was activated in *dgd1*. Quantitative RT-PCR analyses showed that levels of mRNAs coding for two JA-responsive genes, *VSP1* and *PDF1.2*, and for a JA biosynthesis gene, *LOX2*, were all highly upregulated in both 10- and 20-d-old *dgd1-1* mutant seedlings (Figure 2). We then measured the content of various major oxylipins in these plants. As shown in Figure 3, after 10 d of growth, both *dgd1* mutant alleles already had high OPDA levels compared with the wild type, and at day 20, the difference increased markedly and high levels of dn-OPDA, JA, and JA-Ile were also seen in the mutants.

Mutations in Genes Involved in JA Biosynthesis or Signaling Can Rescue the Short Inflorescence Stem and Phloem Cap Lignification Phenotypes of *dgd1*

To examine whether the *dgd1* visible phenotypes and phloem cap cell lignification were caused by activation of the JA signaling pathway, we crossed the *dgd1-1* mutant with a *coi1* mutant (the *coi1-30* allele produced by T-DNA insertion [SALK_035548]; Mosblech et al., 2011; Yang et al., 2012) and found that the *coi1-30 dgd1-1* double mutant had the same general appearance as the *coi1-30* single mutant (Figure 4A). Furthermore, inflorescence stem cross sections showed that phloem cap cells in the double mutant were also not lignified (Figure 4B). To exclude the possibility that the rescue by the *coi1* mutation was due to inactivation of some JA-independent COI1 activity, we also crossed the *dgd1-1* and *dgd1-2* mutants with an AOS knockout mutant (von Malek et al., 2002) and found that the short inflorescence stem, ruffled leaf (Figure 4C), and lignified phloem cap cell (Figure 4D) phenotypes were absent in the *aos dgd1-1* and *aos dgd1-2* double mutants, showing that blocking JA biosynthesis resulted in

Table 1. Galactolipid Composition of the Wild Type and Various Mutants

Plant	MGDG	DGDG
Wild type	33.5 ± 8.3	6.2 ± 1.4
<i>aos</i>	30.5 ± 8.9	5.8 ± 1.2
<i>coi1-30</i>	30.6 ± 5.6	6.1 ± 1.0
<i>dgd1-1</i>	28.4 ± 3.8	0.5 ± 0.2
<i>dgd1-2</i>	24.0 ± 3.4	0.4 ± 0.04
<i>aos dgd1-1</i>	29.1 ± 3.5	0.5 ± 0.1
<i>aos dgd1-2</i>	31.9 ± 4.3	0.5 ± 0.2
<i>coi1-30 dgd1-1</i>	31.0 ± 5.4	0.6 ± 0.1

Plants were grown on 16-h-light/8-h-dark cycles for 10 d on MS plates and then transferred to soil for another 10 d. Means ± SE of at least three independent plant batches are shown. Values are relative peak areas (%).

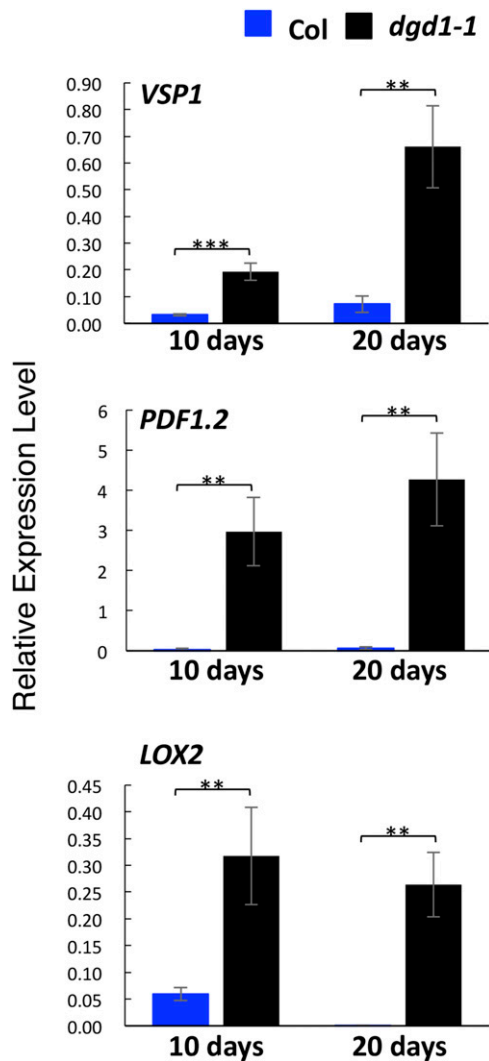


Figure 2. JA Biosynthesis and Signaling Genes Are Highly Activated in the *dgd1-1* Mutant.

Plants were grown on MS plates for 10 d, then one set was harvested and the other was moved to soil and grown for another 10 d. Total RNA was then isolated, and the levels of expression of the three indicated genes were analyzed by quantitative RT-PCR and expressed relative to *UBQ10* gene expression. Means \pm SE for three independent plant batches are shown. Significance levels are as follows: ** $P < 0.01$ and *** $P < 0.001$ (Student's *t* test). Col, wild-type ecotype Columbia.

a general alleviation of most *dgd1* visible phenotypes. However, further quantifications are required to assess if all growth defects are fully rescued.

We then measured oxylipin levels in the double mutants. As shown in Figure 3, the 20-d-old *aos dgd1* double mutants showed no OPDA- or dn-OPDA-related oxylipin production, but, interestingly, in the 20-d-old *coi1-30 dgd1-1* double mutant, high levels of JA and JA-Ile accumulated, showing that JA was overproduced even in the absence of COI1 for positive feedback induction of JA biosynthesis. However, no accumulation of OPDA or

dn-OPDA occurred in the *coi1-30 dgd1-1* double mutant, showing that the high-level accumulation of OPDA and dn-OPDA observed in the *dgd1* single mutants was COI1-dependent.

Lipidomics Analyses of the Mutants

We next performed detailed lipidomics analyses to verify that rescue of the *dgd1* visible phenotypes was not due to the *coi1* and *aos* mutations somehow increasing the DGDG content in the double mutants. As shown in Table 1, the *aos* and *coi1-30* single mutants had the same MDGD and DGDG contents as the wild type (for all lipids analyzed, see Supplemental Table 1), whereas all three double mutants, *aos dgd1-1*, *aos dgd1-2*, and *coi1-30 dgd1-1*, which did not show the *dgd1* visible phenotypes, had less than

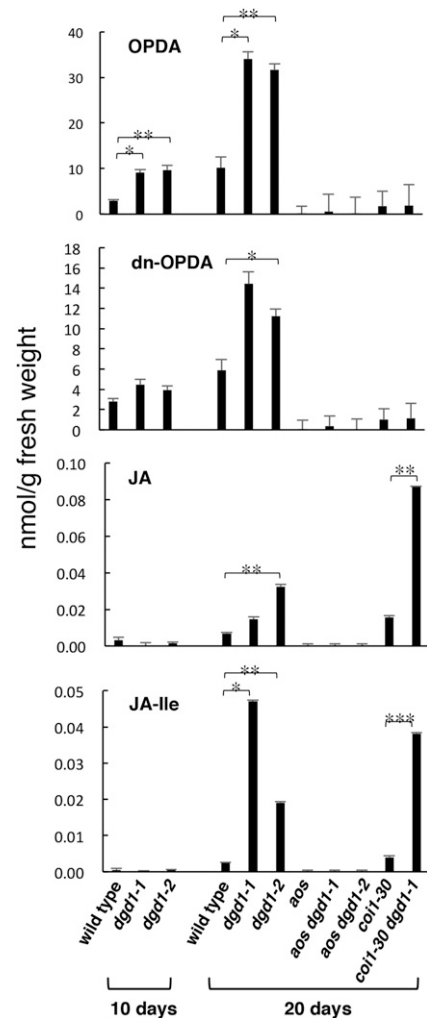


Figure 3. The Two *dgd1* Single Mutants and the *coi1-30 dgd1-1* Double Mutant Have High Oxylipin Levels under Normal Conditions.

Plants were grown on MS plates for 10 d, then one set was harvested and the other was moved to soil and grown for another 10 d, after which the levels of the indicated oxylipins were measured. Means \pm SE for at least three independent plant batches are shown. Significance levels are as follows: * $P < 0.05$, ** $P < 0.01$, and *** $P < 0.001$ (Student's *t* test).

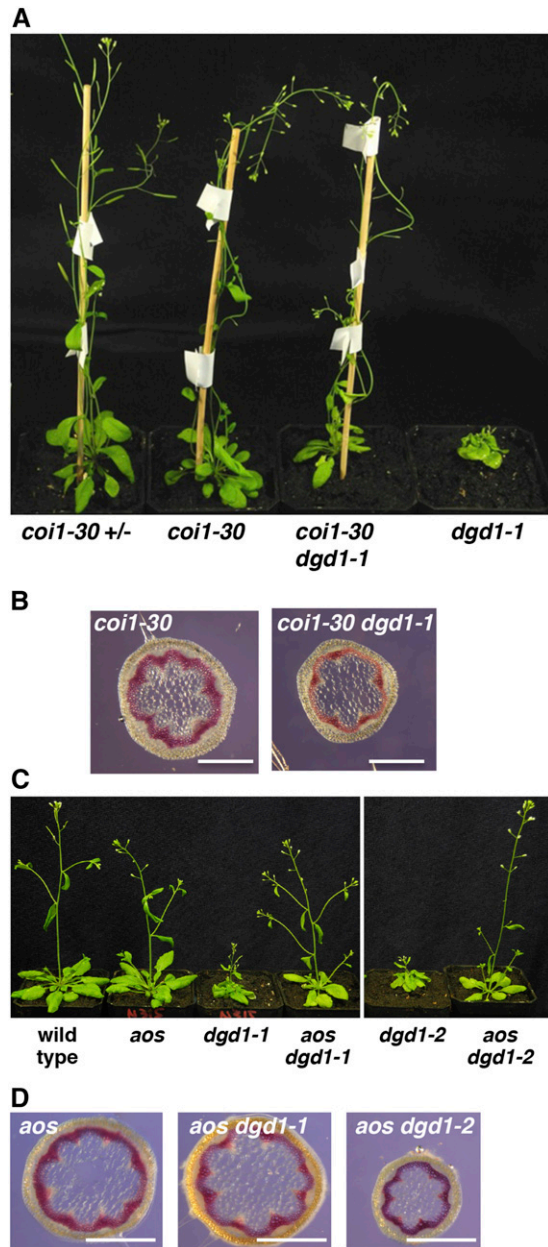


Figure 4. The *coi1 dgd1* and *aos dgd1* Double Mutants No Longer Exhibit the Short Inflorescence Stem and Lignification Phenotypes.

(A) Plants of the indicated genotypes after 40 d of growth; the *coi1-30* heterozygous plant (*coi1-30 +/-*) was used as a wild-type control.

(B) Plants of the indicated genotypes were grown for 40 d, then inflorescence stem cross sections were stained with phloroglucinol. Bars = 0.5 mm.

(C) Plants of the indicated genotypes after 31 d of growth.

(D) Plants of the indicated genotypes were grown for 35 d, then inflorescence stem cross sections were stained with phloroglucinol. Bars = 0.5 mm.

10% of wild-type DGDG levels. In addition, when we analyzed the fatty acid compositions of the lipids (Table 2; Supplemental Data Set 1), the three double mutants and the two *dgd1* single mutants were found to have decreased MGDG (16:3/18:3) levels and increased MGDG (18:3/18:3) levels (Table 2), similar to previously reported findings for *dgd1-1* (Xu et al., 2008).

We also measured the profiles of arabinosides, which are galactolipids containing up to three OPDA and/or dn-OPDA molecules. Arabinosides are present at very low levels under normal growth conditions, and it has been reported that, upon wounding, the most abundant arabinoside is arabinoside A (MGDG esterified with one OPDA moiety and one dn-OPDA moiety) (Kourtchenko et al., 2007; Ibrahim et al., 2011; Vu et al., 2012). As shown in Figure 5, in the absence of wounding and under normal growth conditions, all arabinoside forms were present at very low levels in the wild type, whereas in the *dgd1* single mutants, high levels of both arabinoside B (MGDG esterified with two OPDA) and arabinoside A were seen, with arabinoside B levels being higher than arabinoside A levels. Even levels of arabinoside G (MGDG esterified with three OPDA), which are normally extremely low, were increased significantly in the *dgd1* mutants. This result is in agreement with the *dgd1* mutants having higher levels of MGDG (18:3/18:3) than MGDG (16:3/18:3) (Table 2) and suggests that some excess MGDG may be converted into the corresponding arabinosides in the *dgd1* mutants. In addition, arabinoside levels were not increased in the *coi1-30 dgd1-1* double mutant, showing that, like the high-level accumulation of OPDA and dn-OPDA, the much higher arabinoside levels in the *dgd1* single mutants are COI1-dependent.

Reduced Photosynthesis and Altered Chloroplast Morphology Are Not Caused by Increased JA Levels

Although the *coi1-30 dgd1-1*, *aos dgd1-1*, and *aos dgd1-2* double mutants no longer exhibited short inflorescence stems and ruffled leaves, their leaves still appeared pale green, like the *dgd1* single mutants. Therefore, we measured the chlorophyll content (Figure 6A) and PSII quantum yield (Figure 6B) and found that both were reduced in the single and double mutants compared with the wild type.

Another major phenotype reported for the *dgd1-1* mutant is altered chloroplast morphology. When observed by electron microscopy, instead of being spindle-shaped, like wild-type chloroplasts, *dgd1-1* chloroplast envelopes are usually more rounded, but the thylakoids remain elongated, resulting in bent thylakoids and large thylakoid-free stromal areas (Dörmann et al., 1995; Hölzl et al., 2009). As shown in Figure 7, the *dgd1-2* allele showed the same phenotype as the *dgd1-1* allele, whereas chloroplasts in the *aos* and *coi1-30* mutants had the same morphology as the wild-type chloroplasts, and all double mutants exhibited rounded chloroplasts with bent thylakoids, as in the *dgd1* mutants. This result shows that the altered chloroplast morphology in *dgd1* is not rescued by eliminating JA signaling or production.

Altered Chloroplast Morphology in the *vipp1* Mutant Does Not Elicit a JA Response

Our results showed that, in *dgd1* mutants, activation of JA signaling caused the visible phenotypes but not the altered

Table 2. Fatty Acid Compositions of the Major Forms of MGDG and DGDG

Plant	MGDG (16:3/18:3)	MGDG (18:3/18:3)	DGDG (16:3/18:3)	DGDG (18:3/18:3)
Wild type	13.1 ± 3.1	12.5 ± 3.6	0.50 ± 0.06	4.1 ± 1.1
<i>aos</i>	13.1 ± 4.1	10.1 ± 3.1	0.64 ± 0.11	3.8 ± 0.8
<i>coi1-30</i>	13.3 ± 2.4	10.7 ± 1.6	0.66 ± 0.05	4.1 ± 0.7
<i>dgd1-1</i>	6.3 ± 1.6	17.2 ± 1.8	0.05 ± 0.03	0.3 ± 0.2
<i>dgd1-2</i>	5.6 ± 1.4	13.7 ± 1.9	0.05 ± 0.01	0.3 ± 0.03
<i>aos dgd1-1</i>	8.3 ± 0.7	16.5 ± 2.2	0.08 ± 0.005	0.4 ± 0.1
<i>aos dgd1-2</i>	7.8 ± 0.1	18.4 ± 2.7	0.06 ± 0.03	0.4 ± 0.2
<i>coi1-30 dgd1-1</i>	8.4 ± 0.5	17.9 ± 4.2	0.08 ± 0.02	0.4 ± 0.05

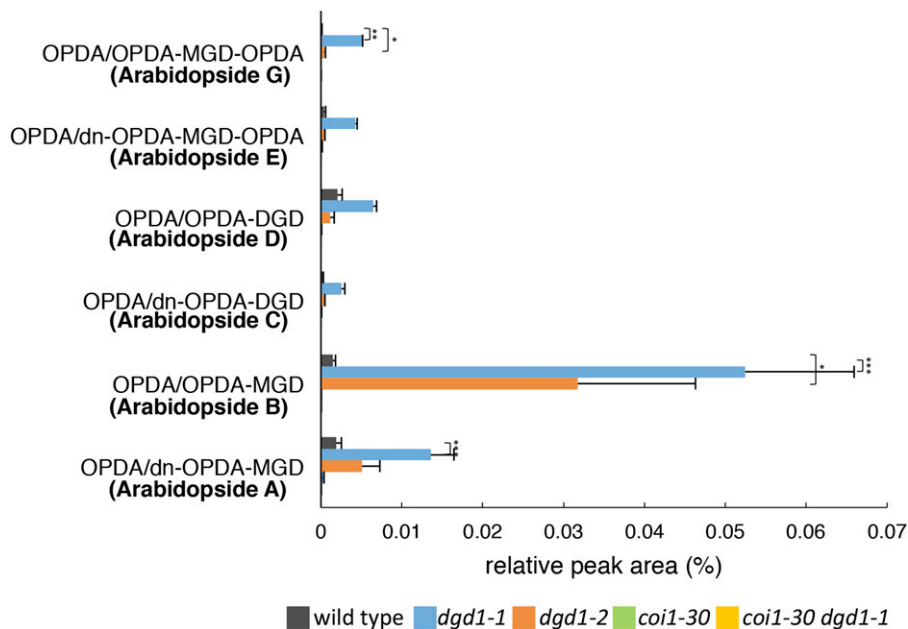
Plants were grown on 16-h-light/8-h-dark cycles for 10 d on MS plates and then transferred to soil for another 10 d. Means ± SE of at least three independent plant batches are shown. Values are relative peak areas (%).

chloroplast morphology. However, it was still possible that the altered chloroplast morphology resulted in a stress condition that induced JA production in the *dgd1* mutants. Therefore, we examined this possibility by analyzing another mutant with a similar altered chloroplast morphology. The *vipp1* (*vesicle-inducing protein in plastids1*) knockdown mutant has rounded chloroplasts with bent thylakoid membranes and large thylakoid-free stromal areas (Zhang et al., 2012), features very similar to those in the *dgd1* mutants. For our analyses of the *dgd1* mutants shown in Figure 7, plants were grown on Murashige and Skoog (MS) plates for 10 d and then moved to soil for another 16 d. For analyses of the *vipp1* mutants, *vipp1* and *dgd1-2* plants were also grown for 26 d but on MS plates throughout, as the *vipp1* knockdown mutant cannot survive on soil (Zhang et al., 2012). Under these conditions, the *dgd1-2* mutant still showed altered chloroplast morphology

(Figure 8A) and activation of the JA-responsive genes *VSP1*, *PDF1.2*, and *LOX2* (Figure 8B), whereas the *vipp1* knockdown mutant plants showed a similarly altered chloroplast morphology but no induction of expression of the JA-responsive genes. These data suggest that OPDA and JA overproduction in the *dgd1* mutants is not caused by altered chloroplast morphology.

JA Biosynthesis Might Be Initially Activated through Increased Levels of Transcripts of *PLA-Iγ3* and *LOXs*

To further understand how JA biosynthesis is activated in the *dgd1* mutants, we analyzed the levels of mRNAs for genes encoding enzymes involved in the first three chloroplast-localized steps of JA biosynthesis, namely linoleate 13-LOX (*LOX2*, *LOX3*, *LOX4*, and *LOX6*), AOS, and AOC (*AOC1* to *AOC4*). We also analyzed the

**Figure 5.** The Two *dgd1* Single Mutants, but Not the *coi1-30 dgd1-1* Double Mutant, Have Increased Levels of Arabidopsides.

Plants were grown on MS plates for 10 d and then moved to soil for another 10 d, after which the levels of the five major arabidopsides were measured. Means ± SE for at least three independent plant batches are shown. Results for plants with the *aos* mutation were close to the detection limits and are not shown. Significance levels are as follows: *P < 0.05, **P < 0.01, and ***P < 0.001 (Student's *t* test).

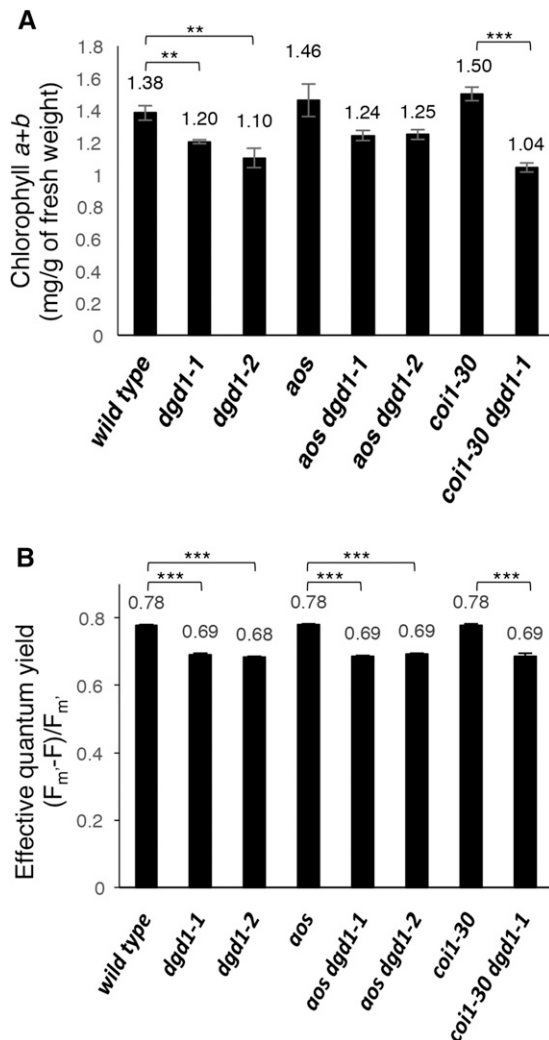


Figure 6. The *coi1-30 dgd1-1* and *aos dgd1* Double Mutants Still Have Reduced Chlorophyll Levels and Photosynthetic Capacity.

(A) Plants were grown on MS plates for 20 d, then leaves were harvested for chlorophyll determination.

(B) Plants were grown on MS plates for 10 d, then the PSII quantum yield was measured.

Means \pm SE for at least three independent plant batches are shown. Significance levels are as follows: ** $P < 0.01$ and *** $P < 0.001$ (Student's t test).

levels of mRNAs coding for the seven class I phospholipase A₁ (PLA₁) members, including *DEFECTIVE IN ANTHOR DEHISCENCE1* (*DAD1*; Ishiguro et al., 2001) and *DGL* (Hyun et al., 2008). Class I PLA₁ members have a predicted chloroplast-targeting transit peptide and are implicated in generating the 18:3 fatty acid serving as the substrate for 13-LOX (Ishiguro et al., 2001; Seo et al., 2009; Ellinger et al., 2010). We measured transcript levels in the wild type, the *dgd1-1* and *coi1-30* single mutants, and the *coi1-30 dgd1-1* double mutant, as comparison of the gene expression profile of the *coi1-30 dgd1-1* double mutant with that of the *dgd1-1* single mutant would allow us to distinguish the

immediate responses caused by the *dgd1* mutation from the subsequent responses induced by the COI1-mediated positive feedback loop. As shown in Figure 9A, transcript levels for the four LOX genes were all slightly higher in the *coi1-30 dgd1-1* double mutant than in the *coi1-30* single mutant, the increases in LOX3 and LOX4 transcript levels being significant. Transcript levels for all four genes were markedly higher in the *dgd1-1* single mutant than in the wild type or the *coi1-30 dgd1-1* double mutant, suggesting that the *dgd1* mutation initially resulted in a slight induction and that the COI1-mediated positive feedback loop resulted in a further induction of LOX gene expression. AOC1 transcript levels in the *dgd1-1* single mutant were increased in a COI1-dependent manner, but no significant induction of expression of the other AOCs or the AOS gene was seen. Interestingly, of the transcript levels for the seven class I PLAs, only those for PLA-I γ 3 were increased significantly in the *dgd1-1* and *coi1-30 dgd1-1* mutants. The increase was actually higher in the *coi1-30 dgd1-1* double mutant, suggesting that PLA-I γ 3 activation was due to the *dgd1* mutation and not related to COI1. When the activity of the seven class I PLAs was analyzed previously using MGDG, DGDG, phosphatidylcholine (PC), and triacylglycerol (TAG) as substrates, PLA-I γ 3 was found to have one of the highest activities and to be the only PLA with a high substrate preference for MGDG (Seo et al., 2009). A mutation in this gene reduces basal JA and OPDA levels but had no effect on JA biosynthesis in wounded leaves (Ellinger et al., 2010). These data suggest that, under nonwounded conditions, some MGDG molecules are cleaved by PLA-I γ 3 to release fatty acids that lead to basal JA production.

We then analyzed LOX and AOC protein levels by immunoblotting using rabbit antisera raised against LOX from cucumber (*Cucumis sativus*) lipid bodies or Arabidopsis AOC. Both antisera recognize multiple LOX and AOC forms in Arabidopsis leaves (Hause et al., 2000; Berger et al., 2001; Stenzel et al., 2003). The chloroplast outer membrane protein-import channel Toc75 (Schnell et al., 1994) was also analyzed as a loading control. As

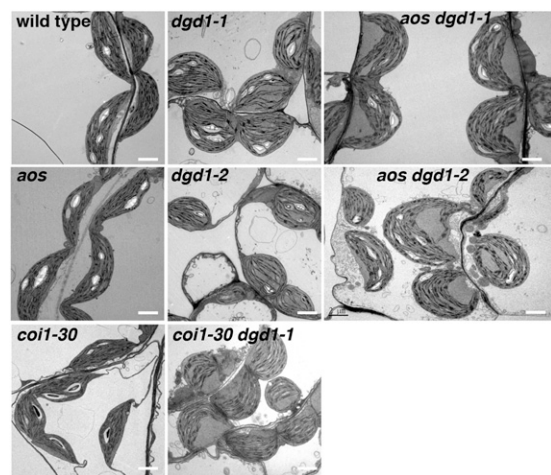


Figure 7. Leaf Chloroplast Morphology of the Wild Type and Various Mutants Shown by Electron Microscopy.

Plants were grown on MS plates for 10 d and then moved to soil for another 16 d. Bars = 2 μ m.

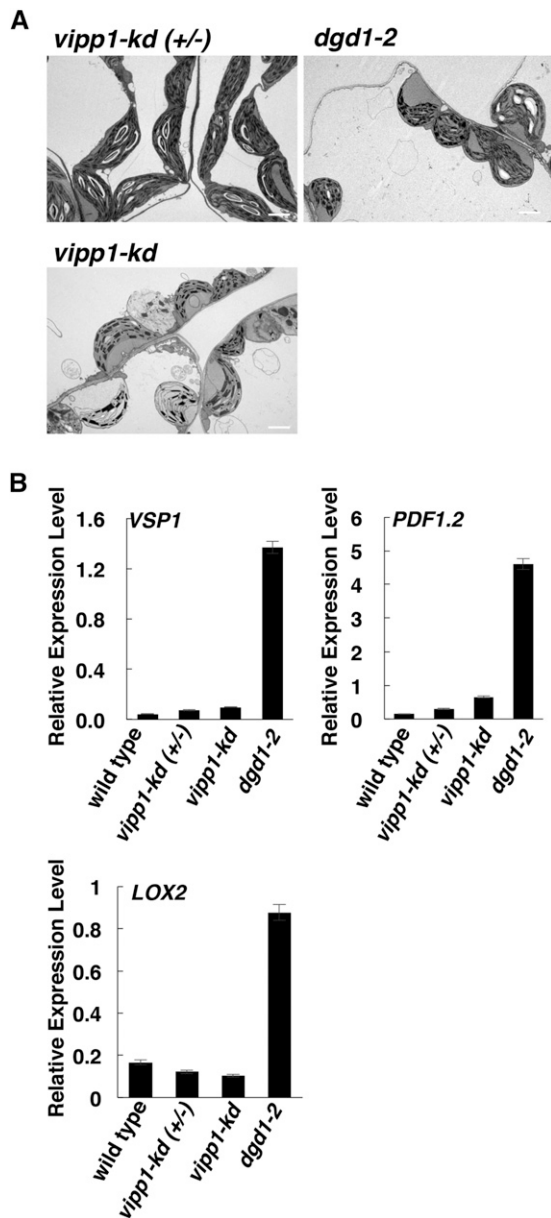


Figure 8. The *vipp1* Knockdown Mutant Shows Altered Chloroplast Morphology but No Activation of JA Signaling.

Plants were grown for 26 d on MS plates, then morphology and JA-responsive gene transcript levels were examined.

(A) Morphology of chloroplasts from *vipp1* knockdown mutant (*vipp1-kd*) plants and heterozygous control [*vipp1-kd (+/-)*] plants. Chloroplasts of *dgd1-2* plants grown under the same conditions are shown for comparison. **(B)** Levels of expression of the JA-responsive genes analyzed by quantitative RT-PCR and normalized to *UBQ10* gene expression. Values are means \pm SD of three technical replicates.

shown in Figure 9B, the *coi1-30* mutation resulted in reduced levels of LOX, as shown previously (Benedetti et al., 1995), and LOX and AOC levels were highly increased in the *dgd1-1* mutant but not in the *coi1-30 dgd1-1* double mutant. These results

suggest that, through the COI1-mediated positive feedback loop, the *dgd1* mutation has induced a high-level stable accumulation of LOX and AOC proteins, which maintained high-level oxylipin production in the mutant plants.

DISCUSSION

Our data show that the *dgd1* mutation leads to JA overproduction, which results in short inflorescence stems and lignification of phloem cap cells. The *aos dgd1* and *coi1-30 dgd1-1* double mutants appeared almost wild type, with only a small reduction in chlorophyll content and photosynthesis, suggesting that, without JA-COI1-mediated growth inhibition, a 90% reduction in DGDG content only has a small effect on plant growth. It is well known that JA inhibits cell cycle progression (Swiatek et al., 2002, 2004; Pauwels et al., 2008; Noir et al., 2013), and growth inhibition is also achieved through crosstalk of JA with other phytohormones, such as auxins, gibberellins, and brassinosteroids (Ren et al., 2009; Kazan and Manners, 2012; Yang et al., 2012). JA also inhibits cell expansion, for example, in petals (Brioudes et al., 2009). In the *dgd1* mutants, JA-COI1-mediated growth inhibition seemed most severe in tissues with vascular bundles; the inflorescence stems were extremely short, while in the leaf, the petioles were very short and the major veins did not elongate sufficiently, but the leaf blade still increased in size, resulting in the ruffled appearance. It is possible that, in addition to suppressed cell division, lignification of the phloem cap cells further restricts the expansion of vascular bundles and pith, resulting in severe inhibition of the elongation of inflorescence stems and major veins. It is not known why oxylipin overproduction causes lignification only in phloem cap cells. Perhaps this group of cells can develop into phloem fibers even in wild-type plants and, therefore, secondary cell wall biosynthesis can be induced more easily in these cells.

MDGD, not DGDG, is suggested to be the primary substrate for arabinoside production because, upon mechanical or freeze-thaw wounding, high levels of arabinosides are seen, in particular those synthesized from MDGD (Ibrahim et al., 2011; Nilsson et al., 2012; Vu et al., 2012). Our data here suggest that, when the major route for the conversion of MDGD to DGDG is blocked by the *dgd1* mutation, some resulting excess MDGD is converted to JA, supporting the idea that, in addition to being a substrate for arabinoside production, MDGD could also be the primary substrate for JA production. In agreement with this suggestion, expression of the gene *MGD1*, coding for the major MGDG synthase, is upregulated by wounding and methyl jasmonate (Kobayashi et al., 2009). However, when rice (*Oryza sativa*) MGDG synthase (OsMGD) was overexpressed in tobacco (*Nicotiana tabacum*), no JA overproduction was observed, but, unlike in the *dgd1* mutants, which have a greatly increased MGDG:DGDG ratio, levels of both MGDG and DGDG were increased in the OsMGD-overexpressing plants, leading to a reduced MGDG:DGDG ratio (Wang et al., 2014). It is likely that, in these OsMGD-overexpressing plants, DGDG biosynthesis was adjusted to maintain the MGDG:DGDG ratio. Interestingly, DGD1 is localized at the outer membrane of plastids, while MGD1 is localized at the inner membrane, and most of the enzymes for OPDA biosynthesis may also be attached to the stromal side of the inner envelope membrane (Froehlich et al.,

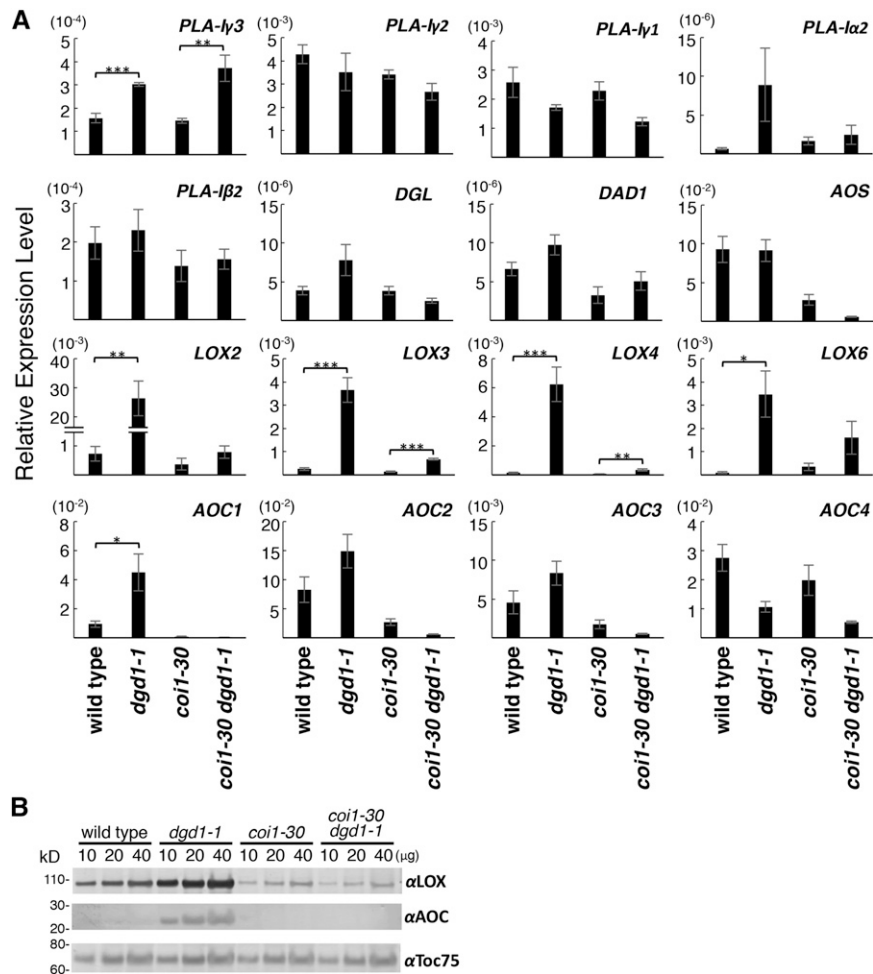


Figure 9. Levels of Expression of Genes Encoding Enzymes for the Initial Steps of JA Biosynthesis.

Plants of the indicated genotypes were grown on MS plates for 10 d, then moved to soil and grown for another 10 d before being harvested for total RNA isolation and protein extraction.

(A) Levels of expression of the indicated genes analyzed by quantitative RT-PCR and expressed relative to *UBQ10* gene expression. Means \pm se for at least three independent plant batches are shown. Significantly higher expression in *dgd1-1* or *coi1-30 dgd1-1* compared with the wild type or *coi1-30*, respectively, is indicated as follows: * $P < 0.05$, ** $P < 0.01$, and *** $P < 0.001$ (Student's *t* test).

(B) Total proteins (10, 20, or 40 μ g, indicated above the lanes) were analyzed by SDS-PAGE, followed by immunoblotting with antiserum against cucumber lipid body LOX, Arabidopsis AOC, or pea Toc75.

2001; Joyard et al., 2010). Conversion of MGDG to DGDG by DGD1, therefore, might rapidly channel some of the MGDG to the outer membrane. This may help in maintaining a correct MGDG:DGDG ratio at the inner membrane and in diverting some MGDG away from the OPDA-synthesizing enzymes and, therefore, may help prevent JA overproduction.

To further understand how JA biosynthesis is activated in the *dgd1* mutants, we measured the transcript levels of genes responsible for the initial steps of JA biosynthesis. Our results showed that *PLA-Iγ3* and *LOX* transcript levels were increased in the *coi1-30 dgd1-1* double mutant. Since LOX catalyzes the first step of oxylipin formation leading to JA biosynthesis, it is reasonable that LOX is the first enzyme to show increased expression when levels of its substrate are increased, as may be the case in

the *dgd1* mutant. While all four *LOX* genes contribute to wound-induced JA formation (Caldelari et al., 2011; Chauvin et al., 2013), they also have different functions. For example, *LOX2* is required to generate the high levels of JA seen proximal to a wound (Schommer et al., 2008; Glauser et al., 2009), and *LOX3* and *LOX4* are required for male fertility (Caldelari et al., 2011). Nonetheless, their responses to the *dgd1* mutation were very similar, all showing a weak induction of expression in the *coi1-30 dgd1-1* double mutant but a very high level of induction in the *dgd1-1* single mutant, although only *LOX3* and *LOX4* transcript levels in the *coi1-30 dgd1-1* double mutant were significantly different from those in the *coi1-30* single mutant. It is possible that the promoters of the *LOX3* and *LOX4* genes may be more responsive to the *dgd1* mutation.

There seem to be stimuli- and pathway-specific lipases to generate fatty acid substrates for JA production, but these have not been clearly identified. DAD1 is required for male fertility but displays a 4-fold higher substrate preference for PC over MGDG (Ishiguro et al., 2001). Overexpression of DGL results in JA overproduction in leaves (Hyun et al., 2008), but DGL shows much higher activity toward DGDG than MGDG (Hyun et al., 2008) and is localized in the cytosol (Ellinger et al., 2010). A knockout mutant of *PLA-I γ 1* reduces initial wound-induced JA formation, but JA levels reach nearly wild-type levels at 60 min after wounding (Ellinger et al., 2010). Our transcript abundance analyses showed that *PLA-I γ 3* was the only PLA gene showing upregulated expression in both the *dgd1-1* and *coi1-30 dgd1-1* mutants. A *PLA-I γ 3* knockout mutant was shown previously to have normal levels of wound-induced JA production but a greater than 50% reduction in basal levels of JA, OPDA, and dn-OPDA (Ellinger et al., 2010), suggesting that lipid cleavage by *PLA-I γ 3* can indeed lead to JA production under normal conditions. Furthermore, *PLA-I γ 3* is the only lipase shown to have a specific substrate preference for MGDG (Seo et al., 2009).

The exact mechanism for the activation of JA biosynthesis in the *dgd1* mutant remains to be investigated. We hypothesize that the increased MGDG:DGDG ratio in *dgd1* chloroplasts may induce an increased level of *PLA-I γ 3*, the lipase with a substrate preference for MGDG. This would result in an initial increase in JA and JA-Ile production, as observed in the *coi1-30 dgd1-1* mutant. However, we have only observed increased *PLA-I γ 3* transcript levels. Whether the protein level and activity of *PLA-I γ 3* are increased in the *dgd1* mutants remain to be investigated. The causal relationship between increased MGDG:DGDG ratio and JA production also needs to be experimentally tested by directly manipulating the MGDG:DGDG ratio and then studying its effect on JA production. Other induction mechanisms for JA biosynthesis also need to be considered. For example, a reduction in DGDG content itself may alter the biophysical properties of the membranes, or the altered chloroplast morphology may trigger stress signals different from that triggered by *vipp1*, and activate the OPDA biosynthesis enzymes.

In the *dgd1* mutant with an intact COI1 positive feedback loop, in addition to the increased levels of *PLA-I γ 3* and *LOX* transcripts seen in the *coi1-30 dgd1-1* mutant, further induction of the expression of *LOX* genes and *LOX* proteins, increased expression of *AOC1* and *AOC* proteins, and accumulation of OPDA, dn-OPDA, and arabidopsides A and B were seen. These increases are most likely the result of positive feedback induction after the COI1-JA-Ile interaction. This may also explain how a small increase in MGDG (18:3/18:3) levels can result in a large increase in OPDA and dn-OPDA production in the *dgd1* mutants, as the small excess of MGDG (18:3/18:3) may only result in the initial increase in JA and JA-Ile levels, as in the *coi1-30 dgd1-1* mutant, but subsequent activation of the COI1 positive feedback loop would result in the further activation of other enzymes in the oxylipin biosynthesis pathway.

It has been shown that replacing DGDG with GGDG in the *dgd1* mutant can restore plant growth and chloroplast shape but not photosynthesis (Hölzl et al., 2006, 2009). Together with our data, this shows that the *dgd1* phenotypes are caused by three factors. First, the reduced photosynthesis and chlorophylls are caused directly by reduced DGDG levels (Hölzl et al., 2006, 2009). Indeed,

DGDG molecules have been found in the crystal structure of cyanobacterial PSII (Guskov et al., 2009). Second, the visible phenotypes of *dgd1* are caused by increased JA levels, as shown in this study. The rescue of visible phenotypes in GGDG-complemented *dgd1* plants (Hölzl et al., 2006, 2009) is most likely due to conversion of the excess MGDG into GGDG, thereby preventing its conversion to JA. Third, the altered chloroplast morphology can be rescued by GGDG but not by blocking JA signaling. MGDG is wedge-shaped and thus has non-bilayer-forming characteristics, whereas DGDG is a bilayer-forming lipid and the MGDG:DGDG ratio may be critical for the shape of chloroplast membranes. It is possible that GGDG can replace DGDG in maintaining chloroplast shape due to its similar bilayer-forming property. Together, these data highlight the many functions of chloroplast membrane lipids and call attention to the need for caution when analyzing phenotypes of chloroplast lipid mutants. GGDG-complemented *dgd1* plants provide an important tool for studying the exact function of the galactose moiety in DGDG. Similarly, the *aos dgd1* double mutants established here could provide a tool for studying the direct effect of reduced DGDG levels on plant growth without activation of the JA signaling pathway.

METHODS

Plant Materials and Growth Conditions

The *Arabidopsis thaliana dgd1-2* mutant allele (SAIL_851_G12) was obtained from the ABRC (<http://abrc.osu.edu/>). The *coi1-30* (SALK_035548; Mosblech et al., 2011; Yang et al., 2012) and *ein2* (SAIL_265_D03) mutants were gifts of Hsu-Liang Hsieh and Long-Chi Wang, respectively. Seeds of *Arabidopsis* were sterilized and plated on MS agar medium containing 2% sucrose and grown in growth chambers with a light intensity of 71 $\mu\text{mol m}^{-2} \text{s}^{-1}$ (cool-white fluorescent light bulbs) and 16-h-light/8-h-dark conditions at 22°C. Unless stated otherwise, in experiments involving adult plants, 10-d-old seedlings were transferred from MS agar plates to soil for further growth. Seeds were obtained from homozygous *aos* mutant plants by spraying the flowers with methyl jasmonate. Seeds from *coi1-30* heterozygous plants and *coi1-30* heterozygous *dgd1-1* homozygous plants were plated, and a small piece of leaf tissue was then cut from each plant for genotyping to identify *coi1-30* homozygous plants and *coi1-30 dgd1-1* double mutant plants. Genotypes of all mutant lines were confirmed by DNA sequencing or genomic PCR using a Phire Plant Direct PCR Kit (Thermo Scientific); the primers used are listed in Supplemental Table 2.

Quantitative RT-PCR and Immunoblot Analyses

Total plant RNA was extracted using TriPure Isolation Reagent (Roche Diagnostics), and genomic DNA contamination was removed with DNase I (Thermo Scientific). First-strand cDNAs were synthesized using Maxima H Minus Reverse Transcriptase (Thermo Scientific) and RNA isolated from seedlings of the indicated age. Quantitative RT-PCR was performed using a LightCycler system (Roche Diagnostics) and a LightCycler-FastStart DNA Master SYBR Green I Kit (Roche Diagnostics). Each PCR mixture contained 50 ng of cDNA and 0.5 mM of each primer pair. The initial denaturing step of 10 min was followed by 30 to 50 PCR cycles of 95°C for 10 s, 60°C for 5 s, and 72°C for 1 s per 25 bp of the expected product. After the PCR, the melting temperature was tested. Quantification was performed using LightCycler 480 software version 1.5.1.62. Normalization was performed using *UBQ10* transcript levels. The primers used are listed in Supplemental Table 2.

For immunoblot studies, the aboveground tissues of 20-d-old seedlings were harvested and snap-frozen in liquid nitrogen and then ground to powder

in liquid nitrogen. Total proteins were extracted and analyzed by SDS-PAGE (NuPAGE 4–12% gradient gel system; Invitrogen) followed by immunoblotting with rabbit antiserum against cucumber (*Cucumis sativus*) lipid body LOX (1:1000 dilution; Hause et al., 2000; Berger et al., 2001), Arabidopsis AOC (1:5000 dilution; Stenzel et al., 2003), or pea (*Pisum sativum*) Toc75 (1:2000 dilution; Tu et al., 2004) and alkaline phosphatase-coupled goat anti-rabbit IgG antibodies (1:5000 dilution; Jackson ImmunoResearch). Bound antibodies were detected using the nitroblue tetrazolium and 5-bromo-4-chloro-3-indolyl phosphate colorimetric system.

Lignin and GUS Staining

Petioles, or inflorescence stems immediately above the rosette leaves, from plants of the indicated age were cut and embedded in 7% agarose. Then, 100- μ m-thick sections were prepared using a vibratome, stained with 5% phloroglucinol-HCl solution (freshly prepared by mixing equal volumes of 10% phloroglucinol in 95% ethanol and 37% HCl), and observed with a dissection microscope with dark-field illumination. For GUS staining of seedlings shown in Supplemental Figure 3, tissues were fixed in 0.3% formaldehyde in 50 mM phosphate buffer, stained with 1 mM X-Gluc in phosphate buffer at 37°C overnight, and cleared in 95% ethanol. Stems from stained seedlings were then cut, embedded, and sectioned as described above.

Hormone and Lipid Analyses

For phytohormone analyses, 100 mg of snap-frozen sample was extracted in a two-phase partitioning system using a mixture of tert-butyl methyl ether:methanol:water (4.2:1.25:1, v/v/v) and analyzed on an HPLC/nano electrospray ionization-tandem mass spectrometry system (Iven et al., 2012). Internal standards were used for quantifications. For lipid analyses, 200 mg of snap-frozen sample was extracted in a mixture of 2-propanol, hexane, and water. Analysis of glycerolipids and nonpolar lipids was performed on an ultra-HPLC-nano electrospray ionization-tandem mass spectrometry system (Tarazona et al., 2015), as described below.

Lipid species were separated using the Acquity UPLC system (Waters) equipped with an Acquity UPLC HSS T3 column (100 mm \times 1 mm, 1 μ m; Waters); aliquots (2 μ L) were injected in partial loop with needle overflow mode at a flow rate of 0.1 mL/min and a separation temperature of 35°C. For chromatography, the following solvent mixtures used: methanol:20 mM ammonium acetate (3:7, v/v) containing 0.1% (v/v) acetic acid (A) and tetrahydrofuran:methanol:20 mM ammonium acetate (6:3:1, v/v/v) containing 0.1% (v/v) acetic acid (B). Different linear binary ultra-HPLC elution gradients were used for the different lipid classes. For all lipids except TAG, elution was performed using a start condition of 65% B for glycerolipid analysis, 80% B for lysolipid analysis, and 50% B for DAG analysis maintained for 2 min, followed by a linear increase to 100% B over 8 min, then 100% B for 2 min, followed by reequilibration to start conditions over 4 min. For TAG, 100% B was used and the chromatographic run was for 8 min.

Chip-based nano electrospray ionization was achieved using a TriVersa Nanomate (Advion) with 5- μ m i.d. nozzles at a flow rate of 218 nL/min and a voltage of 1.3 kV. The electrospray current was set to 70 nA, and the ions were infused into a 4000 QTRAP tandem mass spectrometer (AB Sciex). Targeted molecular species analysis was performed in multiple reaction monitoring mode. Target precursor ions were $[M+NH_4]^+$ for DAG, TAG, and arabidopsides; $[M-H]^-$ for phosphatidylethanolamine, phosphatidylglycerol, phosphatidylinositol, phosphatidylserine, and sulphoquinovosyldiacylglycerol, including their lyso species; and $[M-H+CH_3CO_2H]^-$ for PC, MGDG, and DGDG, including their lyso species. For all lipid species except arabidopsides, the target single reaction monitoring (SRM) transitions were diagnostic for the molecular species acyl chain composition, either by a fatty acid-associated neutral loss in positive ion mode (nonpolar lipids) or by the formation of fatty acyl-related fragments in negative ion

mode (glycerolipids). For arabidopsides, target SRM transitions were diagnostic for the molecular species head groups by the formation of head group-related fragments in positive ion mode (Ibrahim et al., 2011). The dwell time was 20 ms for all SRM transitions. Ion focusing and collision energy were optimized to maximize detector response.

Chlorophyll and Photosynthesis Measurements

Chlorophyll content was measured as described previously (Lichtenthaler, 1987). All measurements were performed in triplicate using three independent batches of 20-d-old plant samples. Chlorophyll fluorescence was determined using the IMAGING-PAM MAXI version chlorophyll fluorometer (Walz). To determine the effective PSII quantum yield, fluorescence emissions F_m' and F of 10-d-old light-adapted (71 μ mol m⁻² s⁻¹) seedlings on MS agar medium were measured, and the quantum yield was calculated as $(F_m' - F)/F_m'$.

Transmission Electron Microscopy

Leaves from 26-d-old plants were cut into 1- \times 1-mm pieces that were then fixed in a solution of 2.5% glutaraldehyde and 4% paraformaldehyde for 4 h, washed with 0.1 M sodium cacodylate, and fixed with 1% OsO₄ for another 1 h. The samples were dehydrated in graded concentrations of ethanol (30, 50, 70, 85, 95, and 100%), transferred to 1,2-propylene oxide, and infiltrated with a series of EPON 812 (EMS) solutions (25, 50, 75, and 100% in 1,2-propylene oxide). The resin was polymerized at 70°C for 16 h and sectioned. Images of the chloroplast structure were observed and captured using a Tecnai G2 Spirit TWIN electron microscope (FEI) and DigitalMicrograph acquisition software (Gatan).

Accession Numbers

Sequence data for this article can be found in the GenBank/EMBL data libraries under the following accession numbers: DGD1 (At3g11670), LOX2 (At3g45140), PDF1.2 (At5g44420), COI1 (At2g39940), AOS (At5g42650), CESA3 (At5g05170), eRF1 (At5g47880), ELP1 (At1g05850), WRKY12 (At2g44745), DET3 (At1g12840), CPK28 (At5g66210), EBP (At3g16770), ETR2 (At3g23150), DAD1 (At2g44810), DGL (At1g05800), PLA-I γ 3 (At1g51440), PLA-I γ 2 (At2g30550), PLA-I γ 1 (At1g06800), PLA-I β 2 (At4g16820), and PLA-I α 2 (At2g31690).

Supplemental Data

Supplemental Figure 1. Visible Phenotypes of the Wild Type and the Two *dgd1* Mutants.

Supplemental Figure 2. Expression of Genes, Mutation of Which Results in Ectopic Lignification.

Supplemental Figure 3. The *dgd1* Phenotypes Are Not Caused by Activation of Auxin or Ethylene Signaling.

Supplemental Table 1. Lipid Composition of the Wild Type and Various Mutant Plants.

Supplemental Table 2. Primers Used for Quantitative RT-PCR and Genotyping.

Supplemental Data Set 1. Fatty Acid Composition of All Lipids Analyzed.

ACKNOWLEDGMENTS

We thank Su-Ping Tsay for assistance with electron microscopy, Wataru Sakamoto for providing *vipp1* knockdown mutant seeds, Hsu-Liang Hsieh for providing *coi1-30* mutant seeds, Long-Chi Wang for providing *ein2*

mutant (SAIL_265_D03) seeds, Bettina Hause for providing the antiserum against Arabidopsis AOC and the IMB English Editing Core, and Tom Barkas for English editing. This work was supported by the Ministry of Science and Technology, Taiwan (Grants NSC100-2321-B-001-011, NSC101-2918-I-001-012, and MOST104-2321-B-001-021 to H.-m.L.), and Academia Sinica of Taiwan (to H.-m.L.).

AUTHOR CONTRIBUTIONS

H.-m.L. and I.F. designed the research. H.-m.L., Y.-T.L., L.-J.C., and C.H. performed the experiments. H.-m.L., Y.-T.L., L.-J.C., C.H., and I.F. analyzed the data. H.-m.L. wrote the article.

Received November 30, 2015; revised December 23, 2015; accepted December 30, 2015; published December 31, 2015.

REFERENCES

- Acosta, I.F., and Farmer, E.E.** (2010). Jasmonates. The Arabidopsis Book 8: e0129, doi/10.1199/tab.0129.
- Altamura, M., Marco Possenti, M., Antonella Matteucci, A., Simona Baima, S., Ida Ruberti, I., and Morelli, G.** (2001). Development of the vascular system in the inflorescence stem of Arabidopsis. *New Phytol.* **151**: 381–389.
- Benedetti, C.E., Xie, D., and Turner, J.G.** (1995). Coi1-dependent expression of an Arabidopsis vegetative storage protein in flowers and siliques and in response to coronatine or methyl jasmonate. *Plant Physiol.* **109**: 567–572.
- Berger, S., Weichert, H., Porzel, A., Wasternack, C., Kühn, H., and Feussner, I.** (2001). Enzymatic and non-enzymatic lipid peroxidation in leaf development. *Biochim. Biophys. Acta* **1533**: 266–276.
- Boudière, L., Michaud, M., Petroustos, D., Rébeillé, F., Falconet, D., Bastien, O., Roy, S., Finazzi, G., Rolland, N., Jouhet, J., Block, M.A., and Maréchal, E.** (2014). Glycerolipids in photosynthesis: composition, synthesis and trafficking. *Biochim. Biophys. Acta* **1837**: 470–480.
- Brioudes, F., Joly, C., Szécsi, J., Vauud, E., Leroux, J., Bellvert, F., Bertrand, C., and Bendahmane, M.** (2009). Jasmonate controls late development stages of petal growth in *Arabidopsis thaliana*. *Plant J.* **60**: 1070–1080.
- Brüx, A., Liu, T.Y., Krebs, M., Stierhof, Y.D., Lohmann, J.U., Miersch, O., Wasternack, C., and Schumacher, K.** (2008). Reduced V-ATPase activity in the trans-Golgi network causes oxylipin-dependent hypocotyl growth inhibition in Arabidopsis. *Plant Cell* **20**: 1088–1100.
- Caldelari, D., Wang, G., Farmer, E.E., and Dong, X.** (2011). Arabidopsis *lox3 lox4* double mutants are male sterile and defective in global proliferative arrest. *Plant Mol. Biol.* **75**: 25–33.
- Caño-Delgado, A., Penfield, S., Smith, C., Catley, M., and Bevan, M.** (2003). Reduced cellulose synthesis invokes lignification and defense responses in *Arabidopsis thaliana*. *Plant J.* **34**: 351–362.
- Chauvin, A., Caldelari, D., Wolfender, J.L., and Farmer, E.E.** (2013). Four 13-lipoxygenases contribute to rapid jasmonate synthesis in wounded *Arabidopsis thaliana* leaves: a role for lipoxygenase 6 in responses to long-distance wound signals. *New Phytol.* **197**: 566–575.
- Dörmann, P., and Benning, C.** (2002). Galactolipids rule in seed plants. *Trends Plant Sci.* **7**: 112–118.
- Dörmann, P., Hoffmann-Benning, S., Balbo, I., and Benning, C.** (1995). Isolation and characterization of an Arabidopsis mutant deficient in the thylakoid lipid digalactosyl diacylglycerol. *Plant Cell* **7**: 1801–1810.
- Ellinger, D., Stingl, N., Kubigsteltig, I.I., Bals, T., Juenger, M., Pollmann, S., Berger, S., Schuenemann, D., and Mueller, M.J.** (2010). DONGLE and DEFECTIVE IN ANOTHER DEHISCENCE1 lipases are not essential for wound- and pathogen-induced jasmonate biosynthesis: Redundant lipases contribute to jasmonate formation. *Plant Physiol.* **153**: 114–127.
- Feussner, I., and Wasternack, C.** (2002). The lipoxygenase pathway. *Annu. Rev. Plant Biol.* **53**: 275–297.
- Fiehn, O., Kopka, J., Dörmann, P., Altmann, T., Trethewey, R.N., and Willmitzer, L.** (2000). Metabolite profiling for plant functional genomics. *Nat. Biotechnol.* **18**: 1157–1161.
- Froehlich, J.E., Itoh, A., and Howe, G.A.** (2001). Tomato allene oxide synthase and fatty acid hydroperoxide lyase, two cytochrome P450s involved in oxylipin metabolism, are targeted to different membranes of chloroplast envelope. *Plant Physiol.* **125**: 306–317.
- Fujii, S., Kobayashi, K., Nakamura, Y., and Wada, H.** (2014). Inducible knockdown of MONOGALACTOSYLDIACYLGLYCEROL SYNTHASE1 reveals roles of galactolipids in organelle differentiation in Arabidopsis cotyledons. *Plant Physiol.* **166**: 1436–1449.
- Fukuda, H.** (2004). Signals that control plant vascular cell differentiation. *Nat. Rev. Mol. Cell Biol.* **5**: 379–391.
- Glauser, G., Dubugnon, L., Mousavi, S.A., Rudaz, S., Wolfender, J.L., and Farmer, E.E.** (2009). Velocity estimates for signal propagation leading to systemic jasmonic acid accumulation in wounded Arabidopsis. *J. Biol. Chem.* **284**: 34506–34513.
- Guskov, A., Kern, J., Gabdulkhakov, A., Broser, M., Zouni, A., and Saenger, W.** (2009). Cyanobacterial photosystem II at 2.9-Å resolution and the role of quinones, lipids, channels and chloride. *Nat. Struct. Mol. Biol.* **16**: 334–342.
- Härtel, H., Lokstein, H., Dörmann, P., Grimm, B., and Benning, C.** (1997). Changes in the composition of the photosynthetic apparatus in the galactolipid-deficient *dgd1* mutant of *Arabidopsis thaliana*. *Plant Physiol.* **115**: 1175–1184.
- Hause, B., Weichert, H., Höhne, M., Kindl, H., and Feussner, I.** (2000). Expression of cucumber lipid-body lipoxygenase in transgenic tobacco: Lipid-body lipoxygenase is correctly targeted to seed lipid bodies. *Planta* **210**: 708–714.
- Hözl, G., Witt, S., Gaude, N., Melzer, M., Schöttler, M.A., and Dörmann, P.** (2009). The role of diglycosyl lipids in photosynthesis and membrane lipid homeostasis in Arabidopsis. *Plant Physiol.* **150**: 1147–1159.
- Hözl, G., Witt, S., Kelly, A.A., Zähringer, U., Warnecke, D., Dörmann, P., and Heinz, E.** (2006). Functional differences between galactolipids and glucolipids revealed in photosynthesis of higher plants. *Proc. Natl. Acad. Sci. USA* **103**: 7512–7517.
- Hyun, Y., et al.** (2008). Cooperation and functional diversification of two closely related galactolipase genes for jasmonate biosynthesis. *Dev. Cell* **14**: 183–192.
- Ibrahim, A., Schütz, A.L., Galano, J.M., Herrfurth, C., Feussner, K., Durand, T., Brodhun, F., and Feussner, I.** (2011). The alphabet of galactolipids in *Arabidopsis thaliana*. *Front. Plant Sci.* **2**: 95.
- Ishiguro, S., Kawai-Oda, A., Ueda, J., Nishida, I., and Okada, K.** (2001). The DEFECTIVE IN ANOTHER DEHISCENCE gene encodes a novel phospholipase A1 catalyzing the initial step of jasmonic acid biosynthesis, which synchronizes pollen maturation, anther dehiscence, and flower opening in Arabidopsis. *Plant Cell* **13**: 2191–2209.
- Iven, T., König, S., Singh, S., Braus-Stromeyer, S.A., Bischoff, M., Tietze, L.F., Braus, G.H., Lipka, V., Feussner, I., and Dröge-Laser, W.** (2012). Transcriptional activation and production of tryptophan-derived secondary metabolites in Arabidopsis roots contributes to the defense against the fungal vascular pathogen *Verticillium longisporum*. *Mol. Plant* **5**: 1389–1402.
- Joyard, J., Ferro, M., Masselon, C., Seigneurin-Berny, D., Salvi, D., Garin, J., and Rolland, N.** (2010). Chloroplast proteomics highlights

- the subcellular compartmentation of lipid metabolism. *Prog. Lipid Res.* **49**: 128–158.
- Kazan, K., and Manners, J.M.** (2012). JAZ repressors and the orchestration of phytohormone crosstalk. *Trends Plant Sci.* **17**: 22–31.
- Kelly, A.A., and Dörmann, P.** (2002). DGD2, an Arabidopsis gene encoding a UDP-galactose-dependent digalactosyldiacylglycerol synthase is expressed during growth under phosphate-limiting conditions. *J. Biol. Chem.* **277**: 1166–1173.
- Kelly, A.A., Froehlich, J.E., and Dörmann, P.** (2003). Disruption of the two digalactosyldiacylglycerol synthase genes DGD1 and DGD2 in Arabidopsis reveals the existence of an additional enzyme of galactolipid synthesis. *Plant Cell* **15**: 2694–2706.
- Kobayashi, K., Nakamura, Y., and Ohta, H.** (2009). Type A and type B monogalactosyldiacylglycerol synthases are spatially and functionally separated in the plastids of higher plants. *Plant Physiol. Biochem.* **47**: 518–525.
- Kourtchenko, O., Andersson, M.X., Hamberg, M., Brunström, A., Göbel, C., McPhail, K.L., Gerwick, W.H., Feussner, I., and Ellerström, M.** (2007). Oxo-phytodienoic acid-containing galactolipids in Arabidopsis: jasmonate signaling dependence. *Plant Physiol.* **145**: 1658–1669.
- Lichtenthaler, H.** (1987). Chlorophylls and carotenoids: pigments of photosynthetic biomembranes. *Methods Enzymol.* **148**: 350–382.
- Matschi, S., Hake, K., Herde, M., Hause, B., and Romeis, T.** (2015). The calcium-dependent protein kinase CPK28 regulates development by inducing growth phase-specific, spatially restricted alterations in jasmonic acid levels independent of defense responses in Arabidopsis. *Plant Cell* **27**: 591–606.
- Matschi, S., Werner, S., Schulze, W.X., Legen, J., Hilger, H.H., and Romeis, T.** (2013). Function of calcium-dependent protein kinase CPK28 of *Arabidopsis thaliana* in plant stem elongation and vascular development. *Plant J.* **73**: 883–896.
- Mosblech, A., Feussner, I., and Heilmann, I.** (2009). Oxylipins: structurally diverse metabolites from fatty acid oxidation. *Plant Physiol. Biochem.* **47**: 511–517.
- Mosblech, A., Thurow, C., Gatz, C., Feussner, I., and Heilmann, I.** (2011). Jasmonic acid perception by CO11 involves inositol polyphosphates in *Arabidopsis thaliana*. *Plant J.* **65**: 949–957.
- Newman, L.J., Perazza, D.E., Juda, L., and Campbell, M.M.** (2004). Involvement of the R2R3-MYB, AtMYB61, in the ectopic lignification and dark-photomorphogenic components of the *det3* mutant phenotype. *Plant J.* **37**: 239–250.
- Nilsson, A.K., Fahlberg, P., Ellerström, M., and Andersson, M.X.** (2012). Oxo-phytodienoic acid (OPDA) is formed on fatty acids esterified to galactolipids after tissue disruption in *Arabidopsis thaliana*. *FEBS Lett.* **586**: 2483–2487.
- Noir, S., Bömer, M., Takahashi, N., Ishida, T., Tsui, T.L., Balbi, V., Shanahan, H., Sugimoto, K., and Devoto, A.** (2013). Jasmonate controls leaf growth by repressing cell proliferation and the onset of endoreduplication while maintaining a potential stand-by mode. *Plant Physiol.* **161**: 1930–1951.
- Pauwels, L., Morreel, K., De Witte, E., Lammertyn, F., Van Montagu, M., Boerjan, W., Inzé, D., and Goossens, A.** (2008). Mapping methyl jasmonate-mediated transcriptional reprogramming of metabolism and cell cycle progression in cultured Arabidopsis cells. *Proc. Natl. Acad. Sci. USA* **105**: 1380–1385.
- Petsch, K.A., Mylne, J., and Botella, J.R.** (2005). Cosuppression of eukaryotic release factor 1-1 in Arabidopsis affects cell elongation and radial cell division. *Plant Physiol.* **139**: 115–126.
- Ren, C., Han, C., Peng, W., Huang, Y., Peng, Z., Xiong, X., Zhu, Q., Gao, B., and Xie, D.** (2009). A leaky mutation in DWARF4 reveals an antagonistic role of brassinosteroid in the inhibition of root growth by jasmonate in Arabidopsis. *Plant Physiol.* **151**: 1412–1420.
- Schnell, D.J., Kessler, F., and Blobel, G.** (1994). Isolation of components of the chloroplast protein import machinery. *Science* **266**: 1007–1012.
- Schommer, C., Palatnik, J.F., Aggarwal, P., Chételat, A., Cubas, P., Farmer, E.E., Nath, U., and Weigel, D.** (2008). Control of jasmonate biosynthesis and senescence by miR319 targets. *PLoS Biol.* **6**: e230.
- Schuetz, M., Smith, R., and Ellis, B.** (2013). Xylem tissue specification, patterning, and differentiation mechanisms. *J. Exp. Bot.* **64**: 11–31.
- Sehr, E.M., Agusti, J., Lehner, R., Farmer, E.E., Schwarz, M., and Greb, T.** (2010). Analysis of secondary growth in the Arabidopsis shoot reveals a positive role of jasmonate signalling in cambium formation. *Plant J.* **63**: 811–822.
- Seo, Y.S., Kim, E.Y., Kim, J.H., and Kim, W.T.** (2009). Enzymatic characterization of class I DAD1-like acylhydrolase members targeted to chloroplast in Arabidopsis. *FEBS Lett.* **583**: 2301–2307.
- Steffen, R., Kelly, A.A., Huyer, J., Dörmann, P., and Renger, G.** (2005). Investigations on the reaction pattern of photosystem II in leaves from Arabidopsis thaliana wild type plants and mutants with genetically modified lipid content. *Biochemistry* **44**: 3134–3142.
- Stenzel, I., Hause, B., Miersch, O., Kurz, T., Maucher, H., Weichert, H., Ziegler, J., Feussner, I., and Wasternack, C.** (2003). Jasmonate biosynthesis and the allene oxide cyclase family of *Arabidopsis thaliana*. *Plant Mol. Biol.* **51**: 895–911.
- Swiatek, A., Azmi, A., Stals, H., Inzé, D., and Van Onckelen, H.** (2004). Jasmonic acid prevents the accumulation of cyclin B1;1 and CDK-B in synchronized tobacco BY-2 cells. *FEBS Lett.* **572**: 118–122.
- Swiatek, A., Lenjou, M., Van Bockstaele, D., Inzé, D., and Van Onckelen, H.** (2002). Differential effect of jasmonic acid and abscisic acid on cell cycle progression in tobacco BY-2 cells. *Plant Physiol.* **128**: 201–211.
- Tarazona, P., Feussner, K., and Feussner, I.** (2015). Enhanced plant lipidomics method based on multiplexed LC-MS reveals additional insights into cold and drought-induced membrane remodeling. *Plant J.* **84**: 621–633.
- Tu, S.L., Chen, L.J., Smith, M.D., Su, Y.S., Schnell, D.J., and Li, H.M.** (2004). Import pathways of chloroplast interior proteins and the outer-membrane protein OEP14 converge at Toc75. *Plant Cell* **16**: 2078–2088.
- Ulmasov, T., Liu, Z.B., Hagen, G., and Guilfoyle, T.J.** (1995). Composite structure of auxin response elements. *Plant Cell* **7**: 1611–1623.
- von Malek, B., van der Graaff, E., Schneitz, K., and Keller, B.** (2002). The Arabidopsis male-sterile mutant *dde2-2* is defective in the ALLENE OXIDE SYNTHASE gene encoding one of the key enzymes of the jasmonic acid biosynthesis pathway. *Planta* **216**: 187–192.
- Vu, H.S., Tamura, P., Galeva, N.A., Chaturvedi, R., Roth, M.R., Williams, T.D., Wang, X., Shah, J., and Welti, R.** (2012). Direct infusion mass spectrometry of oxylipin-containing Arabidopsis membrane lipids reveals varied patterns in different stress responses. *Plant Physiol.* **158**: 324–339.
- Wang, H., Avci, U., Nakashima, J., Hahn, M.G., Chen, F., and Dixon, R.A.** (2010). Mutation of WRKY transcription factors initiates pith secondary wall formation and increases stem biomass in dicotyledonous plants. *Proc. Natl. Acad. Sci. USA* **107**: 22338–22343.
- Wang, S., Uddin, M.I., Tanaka, K., Yin, L., Shi, Z., Qi, Y., Mano, J., Matsui, K., Shimomura, N., Sakaki, T., Deng, X., and Zhang, S.** (2014). Maintenance of chloroplast structure and function by overexpression of the rice *MONOGALACTOSYLDIACYLGLYCEROL*

- SYNTHASE* gene leads to enhanced salt tolerance in tobacco. *Plant Physiol.* **165**: 1144–1155.
- Wasternack, C., and Hause, B.** (2013). Jasmonates: Biosynthesis, perception, signal transduction and action in plant stress response, growth and development. An update to the 2007 review in *Annals of Botany. Ann. Bot. (Lond.)* **111**: 1021–1058.
- Xu, C., Moellering, E.R., Fan, J., and Benning, C.** (2008). Mutation of a mitochondrial outer membrane protein affects chloroplast lipid biosynthesis. *Plant J.* **54**: 163–175.
- Yang, D.L., et al.** (2012). Plant hormone jasmonate prioritizes defense over growth by interfering with gibberellin signaling cascade. *Proc. Natl. Acad. Sci. USA* **109**: E1192–E1200.
- Zhang, L., Kato, Y., Otters, S., Vothknecht, U.C., and Sakamoto, W.** (2012). Essential role of VIPP1 in chloroplast envelope maintenance in *Arabidopsis*. *Plant Cell* **24**: 3695–3707.
- Zhong, R., Ripberger, A., and Ye, Z.H.** (2000). Ectopic deposition of lignin in the pith of stems of two *Arabidopsis* mutants. *Plant Physiol.* **123**: 59–70.